

1 **Supplementary Information**  
2 **Evolutionary history of zoogeographical regions surrounding the Tibetan**  
3 **Plateau**

4

5 **This PDF file includes:**

6       Supplementary Figures 1–5

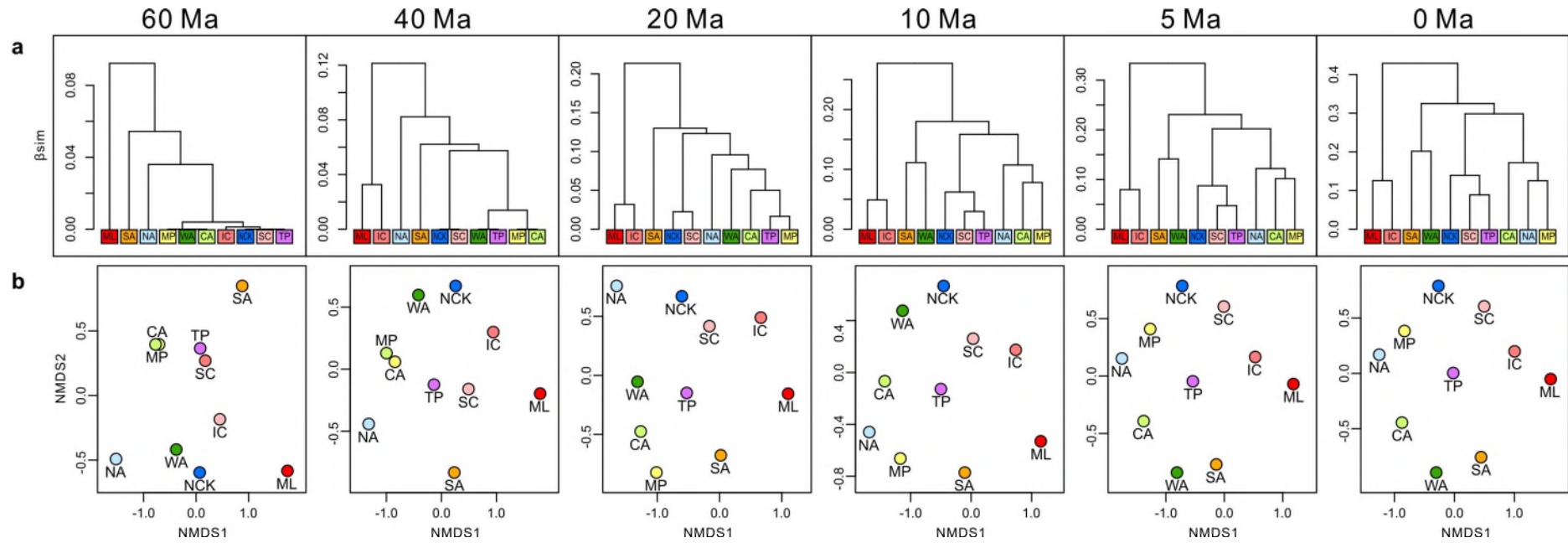
7       Supplementary Tables 1–2

8       Supplementary Methods

9       Supplementary References

10

11 **Supplementary Figures**



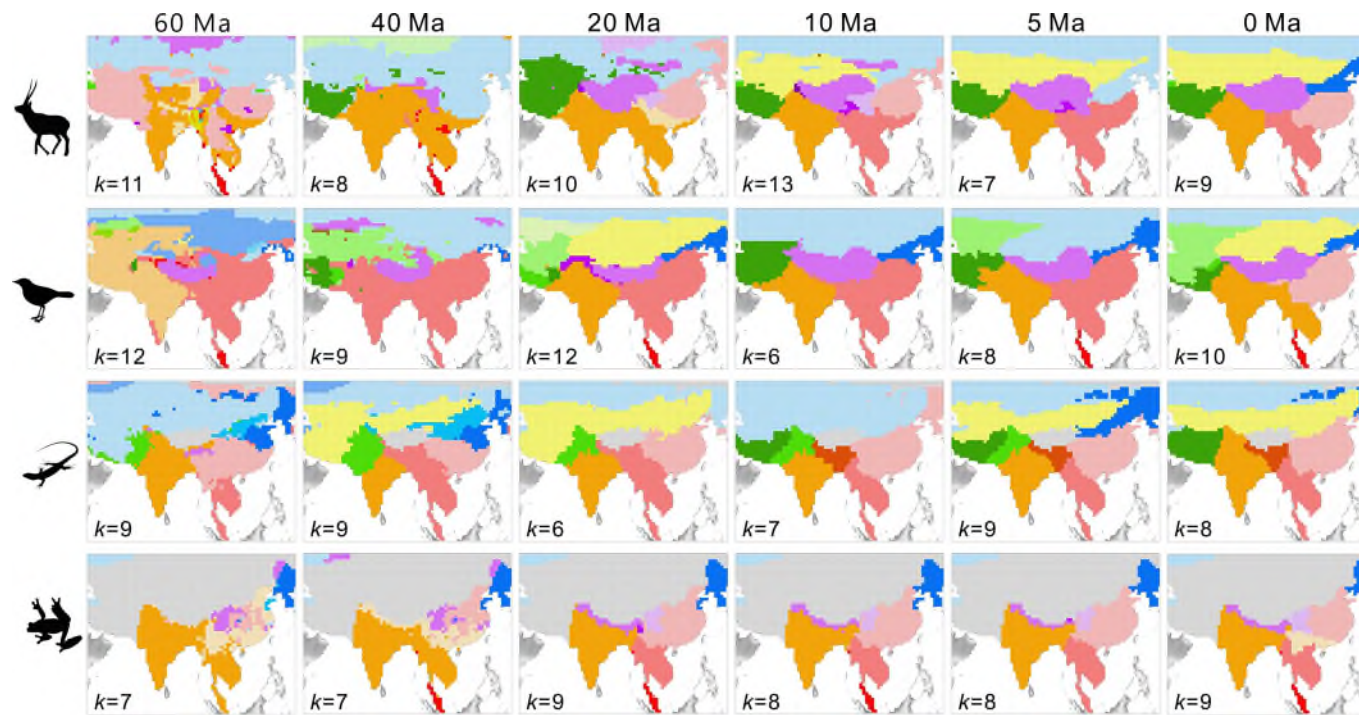
12

13 **Supplementary Figure 1 Temporal changes in zoogeographical regions surrounding the Tibetan Plateau at successive phylogenetic**

14 **depths during the Cenozoic for the whole-region species list of all terrestrial vertebrates. a. Dendrograms plotted by the unweighted**

15 **pair-group method using arithmetic average clustering. b. Non- metric multidimensional scaling ordinations based on the  $\beta_{sim}$  matrices of**

16 **whole-region species list of all terrestrial vertebrates**



17

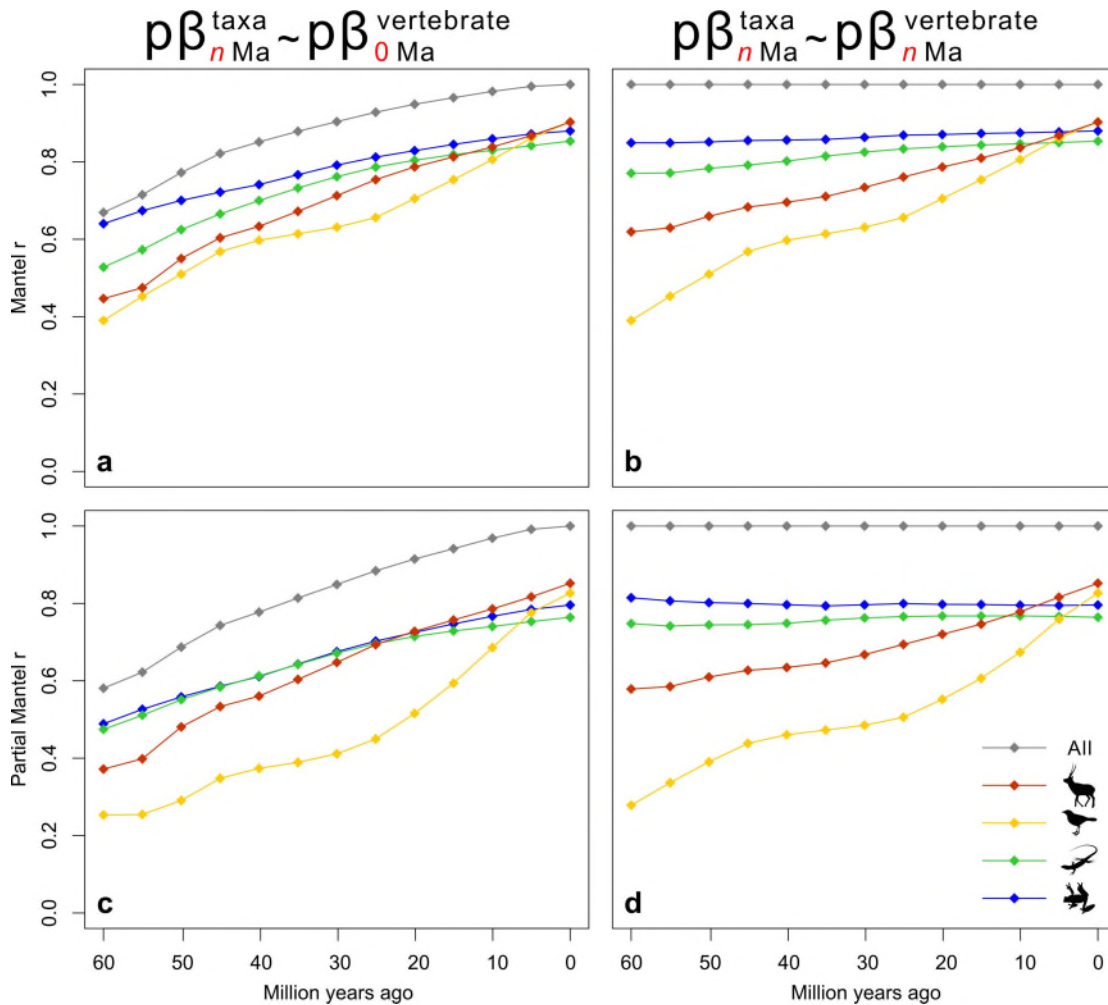
18 **Supplementary Figure 2 Temporal changes in the zoogeographical regions surrounding the Tibetan Plateau at successive phylogenetic**

19 **depths during the Cenozoic for four vertebrate classes.** The zoogeographical regions were generated based on  $p\beta_{sim}$  dissimilarity between

20 pairs of grid-based communities for individual vertebrate classes (mammals, birds, reptiles, and amphibians). The optimal cluster number for

21 each time interval was based on mean silhouette width and explained dissimilarity (Supplementary Data 3). In the amphibian and reptile maps,

22 grid cells with species richness  $< 5$  are in grey.



23

24 **Supplementary Figure 3 Mantel and partial Mantel correlation tests between the**

25  **$\rho\beta_{\text{sim}}$  matrices of each vertebrate class and all terrestrial vertebrates. a. Mantel**

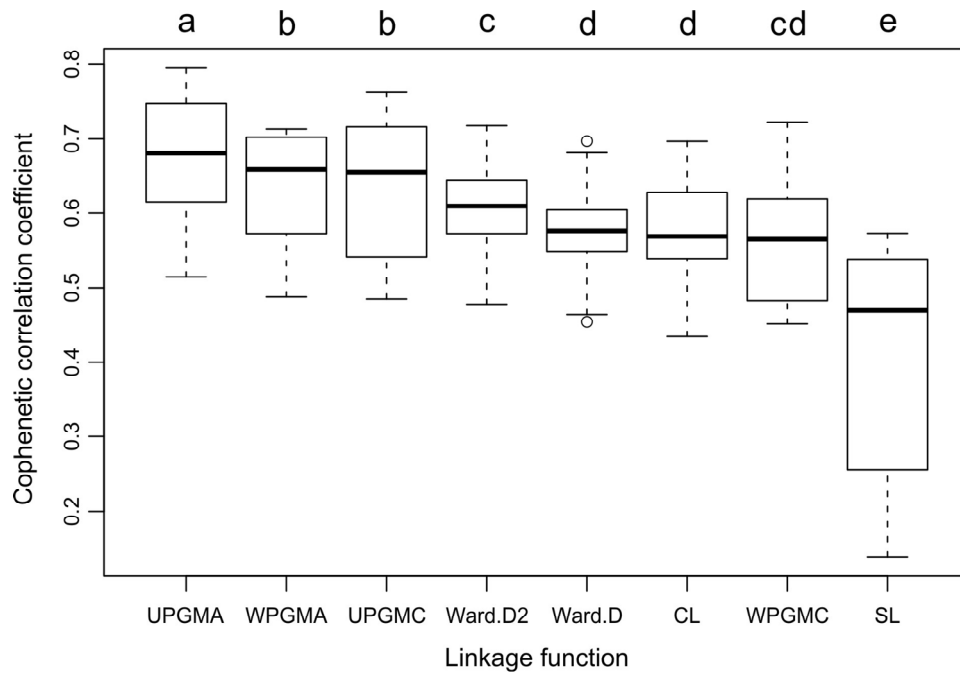
26 correlation tests between each vertebrate class in a given time interval and all

27 terrestrial vertebrates at present. b. Mantel correlation tests between each vertebrate

28 class and all terrestrial vertebrates in a given time interval. c and d. Partial Mantel

29 tests with a matrix of pairwise Euclidean distances as a covariate. All tests were

30 highly significant ( $P < 0.001$ )



31

32 **Supplementary Figure 4** Boxplots showing co-phenetic correlation coefficients of

33 **eight different clustering algorithms across 13 phylogenetic depths from 60 to 0**

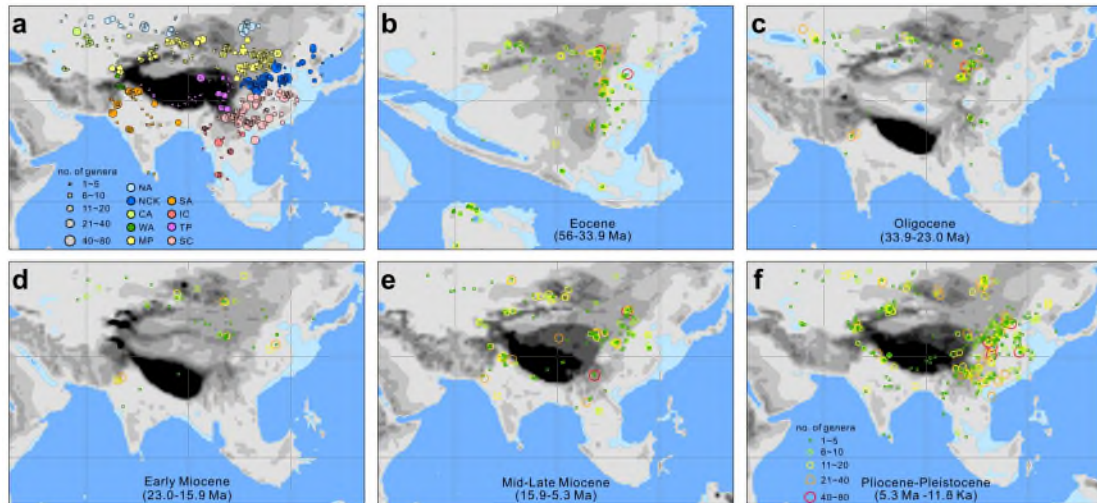
34 **Ma, at intervals of 5 Myr time bins.** Boxes show the median and 25th and 75th

35 percentiles. The letters indicate significant differences among eight clustering

36 algorithms (Wilcoxon Signed Rank Tests,  $P < 0.05$ ).

37

38



39

40 **Supplementary Figure 5 Spatial and temporal distribution of fossil assemblages**

41 **during the Cenozoic. a.** Fossil assemblages with different colors indicating their

42 assignments within different zoogeographical region. **b-f.** Distributions of fossil

43 assemblages during different time periods. The size of the symbol is proportional to

44 the number of mammal genera in each assemblage.

45

46

47 **Supplementary Tables**

48 **Supplementary Table 1** Mantel correlations (Spearman's rho) among pairs of time  
 49 slices based on  $\beta_{\text{sim}}$  matrices at the genus level (below the diagonal). *P* values are  
 50 listed above the diagonal with  $P < 0.05$  in bold. Plio-Pleis: Pliocene–Pleistocene.

Epoch	Present	Plio-Pleis	Mid-Late Miocene	Early Miocene	Oligocene	Eocene
Present	—	<b>0.019</b>	0.053	0.229	0.079	<b>0.022</b>
Plio-Pleis	<b>0.3645</b>	—	<b>0.020</b>	0.987	0.278	<b>0.048</b>
Mid-Late Miocene	0.3490	<b>0.5131</b>	—	<b>0.047</b>	0.145	0.211
Early Miocene	0.1789	-0.5619	<b>0.5139</b>	—	0.357	0.620
Oligocene	0.3048	0.1351	0.2894	0.1423	—	0.393
Eocene	<b>0.4606</b>	<b>0.4796</b>	0.2715	-0.0995	0.0898	—

51

52 **Supplementary Table 2** Proportion of observed genera of the number of those  
 53 expected by the Chao2 estimator for each time interval. The number of fossil localities  
 54 within the zoogeographical regions is in parenthesis. ‘—’, indicates faunas not  
 55 sampled or with fewer than five genera. Plio-Pleis: Pliocene–Pleistocene.

Region	Plio-Pleis	Mid-Late Miocene	Early Miocene	Oligocene	Eocene
Central Asia	63.7(10)	—	28.6(2)	54.1(17)	33.1(2)
Indochina	53.6(14)	35.9(7)	—	100(1)	7.5(12)
Mongolian Plateau	62.4(33)	67.3(36)	56.9(14)	81.3(49)	73(54)
North Asia	76.6(32)	26.8(6)	61.2(4)	100(1)	—
North China & Korea	54.1(64)	55.3(21)	39(4)	38.5(5)	44.3(30)
South Asia	68.8(18)	68.8(12)	7.7(4)	7.3(4)	26.1(7)
South China	68.5(67)	11.7(7)	100(1)	14.5(10)	48.2(35)
Tibetan Plateau	32.3(23)	6.5(8)	21.4(3)	100(1)	50(2)
West Asia	29.2(4)	11.5(3)	—	—	—
Mean±SD (n)	56.6±15.4(265)	41.1±27.5(103)	45±28.5(32)	62±36.3(88)	40.3±19.2(142)

56

57

58

59 **Supplementary Method**

60 *Dissimilarity index*

61 We used Simpson's dissimilarity index ( $\beta_{sim}$ ) and Simpson's phylogenetic  
62 dissimilarity index ( $p\beta_{sim}$ ) to generate pairwise dissimilarity for each pair of  
63 communities (1). These two dissimilarity indices represent species (or phylogenetic)  
64 turnover independent of the total species richness (or branch length) difference  
65 between two communities (2).

66 The  $\beta_{sim}$  index calculates the pairwise species dissimilarity distance between two  
67 communities as follows:

$$\beta_{sim} = 1 - \frac{a}{\min(b, c) + a}$$

68 where  $a$  is the number of shared species and  $b$  and  $c$  are the number of species unique  
69 to each grid cell.  $\beta_{sim}$  ranges from 0 to 1, with smaller values indicating lower  
70 dissimilarity.

71 The  $p\beta_{sim}$  index calculates the pairwise phylogenetic dissimilarity distance between  
72 two grid cells as follows:

$$p\beta_{sim} = \frac{\min(PD_{Total} - PD_k, PD_{Total} - PD_j)}{PD_k + PD_j - PD_{Total} + \min(PD_{Total} - PD_k, PD_{Total} - PD_j)}$$

73 where  $PD_j$  and  $PD_k$  are the total branch lengths of communities  $j$  and  $k$ , respectively.  
74  $PD_{Total}$  is the total branch length of a phylogenetic tree containing all species present  
75 in both communities  $j$  and  $k$ .  $p\beta_{sim}$  ranges from 0 (species are identical and share the  
76 same branch lengths) to 1 (species share no phylogenetic branches).

77



78 *Determining the optimal number of clusters*

79 We implemented the approach of Holt et al. (3) to select suitable dendrogram cutoff  
80 points based on the explained dissimilarity and mean silhouette width. The explained  
81 dissimilarity is the ratio of the sums of mean dissimilarity within different clusters to  
82 the total matrix dissimilarity. This value tends to 1 when all areas are considered as  
83 independent groups. The silhouette width assesses the clustering solutions and ranges  
84 between -1 and +1. A negative silhouette width indicates that most cells are probably  
85 located in an incorrect cluster (4). We only considered the alternate cluster numbers in  
86 the range of 2–15, as many regions were difficult to recognize and explain.

87

88 *Cross-taxon analyses*

89 For four individual vertebrate classes, we generated separate  $p\beta_{sim}$  matrices between  
90 gridded species assemblages at different phylogenetic depths. Similarly, we ran  
91 UPGMA clustering and NMDS ordinations to investigate the changes in assignments  
92 and topologies of clustering dendrograms over a phylogenetic timescale. Besides, we  
93 used Mantel tests to calculate the correlation coefficients of the phylogenetic  
94 dissimilarity matrices ( $p\beta_{sim}$ ) between each vertebrate class and all terrestrial  
95 vertebrates in different time slices. To account for the spatial autocorrelation (i.e.  
96 geographical distance), we repeated these analyses using the partial Mantel tests.  
97 Statistical significance was calculated with a Mantel Carlo permutation test using 999  
98 permutations.

99

100 *Analyses based on whole-region mammal list*

101 Because we merged the fossil records to coarse zoogeographical regions to infer the  
102 changes in fossil assemblages, and to maximize the comparison of fossil data and  
103 molecular phylogeny, we calculated the phylogenetic dissimilarities between  
104 zoogeographical regions based on the species lists for the whole region. In this  
105 analysis, we obtained the whole-region species lists by combining grid cells belonging  
106 to the zoogeographical regions identified by the present-day phylogenetic beta  
107 diversity. Then, we calculated  $p\beta_{sim}$  between each pair of zoogeographical regions at  
108 different phylogenetic depths and performed UPGMA clustering and NMDS  
109 ordinations. Finally, we assessed the differences in the UPGMA dendrograms and  
110 NMDS ordinations based on gridded assemblages versus whole-region species lists.

111

## 112 **Supplementary References**

- 113 1. Baselga, A. Partitioning the turnover and nestedness components of beta diversity.  
114 *Global Ecol. Biogeogr.* **19**, 134-143 (2010).
- 115 2. Leprieur, F. & Oikonomou, A. The need for richness - independent measures of  
116 turnover when delineating biogeographical regions. *J. Biogeogr.* **41**, 417-420  
117 (2014).
- 118 3. Holt, B. G. *et al.* An update of Wallace's zoogeographic regions of the world.  
119 *Science* **339**, 74-78 (2013).
- 120 4. Dapporto, L. *et al.* A new procedure for extrapolating turnover regionalization at  
121 mid-small spatial scales, tested on British butterflies. *Methods Ecol. Evol.* **6**,

